A REVIEW OF RECENT POSITRON ANNIHILATION NDE APPLICATIONS

S. Panchanadeeswaran, Po-We Kao, R. W. Ure, Jr., and J. G. Byrne
Department of Materials Science and Engineering
University of Utah
Salt Lake City, Utah 84112

ABSTRACT

This review will treat two recent applications of positron annihilation to metallurgical studies and will involve the measurement of the Doppler effect associated with the gamma rays emitted during positron annihilation. The applications will be: studies of the interactions of dislocations with pre-precipitates in aged Al-4 weight percent Cu single crystals and studies of the effect of hydrogen charging into polycrystalline nickel.

INTRODUCTION

Earlier[1] it was reported that a commercial aluminum base age hardening alloy, 7075, responded to Doppler broadening measurements by exhibiting higher values of the peak to wings shape parameter for harder conditions. Thus, the Doppler shape factor was behaving in much the same way in which it would respond to plastic deformation in a pure metal; that is, in a pure metal subjected to damage the Doppler peak shape becomes sharper because dislocations and vacancies provide locations for positron trapping which are lacking in ion cores. Hence, positrons attracted to and trapped in such regions will tend more to annihilate with lower energy conduction electrons. Such annihilations cause a smaller Doppler shift from the central energy value of 511 keV than would be caused were the positron to annihilate with a more energetic core electron. Thus, the curve representing the number of annihilations versus plus and minus deviations in annihilation gamma ray energy about a central value of 511 keV (the value if the electron-positron center of mass were stationary) sharpens with rising defect concentration and, conversely, the shape broadens with the annealing out of damage. The gamma rays emitted on annihilation enter a Ge(Li) spectrometer capable of measuring their energy.

RESULTS

To have a better chance of understanding the response of positrons to changes during age hardening[2], we set out to produce well documented aged states in a known alloy; that is, to look at G. P. zones, transition precipitates (θ'), and the equilibrium precipitate (θ) in both single and polycrystalline Al + 4 weight percent Cu alloy. The heat treatments used were: solution treated (S.T.) at 550°C for 1 hour + water quench (Q) for the supersaturated solid solution; S.T. + Q + 130°C for 48 hours for G.P. I zones; S.T. + Q + 190°C for 5 hours for G.P. II zones; S.T. + Q + 240°C for 24 hours for θ'; and S.T. + Q + 400°C for 24 hours + 315°C for 48 hours for θ (the equilibrium precipitate).

When peak to wing (P/W) Doppler comparisons were made, both Na^{22} and Ge^{68} were used as positron sources. The Na^{22} produces positrons with a maximum energy of 0.546 MeV and the Ge^{68} produces positrons with a maximum energy of 1.9 MeV; thus, the former positrons will sample events closer to the specimen surface than the latter positrons.

P/W data for an aged single crystal utilizing a Na^{22} positron source are shown in Fig. 1, plotted against the principal aging temperature. One sees a rise in P/W ratio from the solid solution level to the G.P. zone conditions and a later decline as θ' and θ are formed.

Figure 2 exhibits P/W data taken on the same samples, but with Ge^{68} as the positron source. One sees a similar trend (except for the G. P. II point) in the data, all of which lie in a lower magnitude range. When these experiments were repeated with polycrystalline samples and the Ge^{68} positron source, similar data trends to those of Fig. 2 resulted (with the exception of G. P. II).

A number of conclusions emerge at this point. For the "bulk" data obtained with Ge^{68}, the P/W values for the polycrystals were usually lower point for point than the corresponding values for the single crystal experiments. This would suggest that in the quenched condition fewer point defects are present in the polycrystal because of leakage to grain boundary sinks. In subsequent aging this would lead to a lower density of pre-precipitate nucleation sites in the polycrystal. This would account for the lower P/W ratios in a G. P. zone condition because the coherency strain or hardness of the region measured would be lower.

Again, the case of the G. P. II zone containing single crystal Ge^{68} data violates this scheme. The same data point will later be seen to be at variance with the interpretation given to the θ' condition; that is, it can reasonably be regarded as a bad data point, but for reasons as yet unclear.

For θ' and θ data, the lower nucleation frequency again seems to explain the lower values of P/W ratio for the polycrystalline samples. However, the basis for the values themselves no longer can be ascribed to coherency strains, but rather may be reflective of positron trapping at the θ' and θ matrix-particle interface.

In every case, P/W values measured closer to the surface (Na^{22}) exceeded those measured at greater depths (Ge^{68}). This may be related to the higher quenching rates and point defect concentrations of the surface region which in turn would on aging produce a higher nucleation rate

of precipitation.

Independent of depth, the quenched solid solution was always lower in P/W ratio than either the G. P. zone or overaged conditions. This implies that the stain effect of G. P. zones is much more interactive with positrons than is the discreet point defect distribution created by quenching. The θ' and θ conditions are also more interactive with positrons than is the quenched state--again probably due to interfacial rather than strain field trapping reasons.

In comparing G. P. I and G. P. II zones, it seems (with the one exception previously noted) that the trapping of positrons is greater for the more highly stained G. P. II condition. As one then passes to the partially coherent (less strain) θ' situation, the positrons are less effectively trapped than by the coherent G. P. II particles. Finally, in comparing θ' and θ, it seems that the completely incoherent θ particles have a more effective positron trapping interface than do the θ' particles.

We now proceed to more recent single crystal experiments[3] in which the interaction of various of the above aged states in single crystals respond to tensile deformation. It is known that for G. P. zone states dislocations must rigidly cut through the zones[4], giving the crystal a high yield strength, but a modest rate of work hardening. For the θ' and θ situations, on the other hand, the dislocations bow out between the particles, wrap around, and pass on as in the Fisher-Hart-Pry[5] or Orowan[6] descriptions. The latter produces low initial strength, but a high rate of work hardening as multiple dislocation loops about the particles produce stress fields which resist the approach of new dislocations.

Figure 3 shows plots of Iv (the ratio of peak counts to total counts) and Ic (the ratio of wing counts to total counts) versus tensile strain for a G. P. I zone containing single crystals. The most important feature is that Iv does not change with tensile strain; that is, the cutting of G. P. I zones does not show up in Doppler broadening as would ordinary tensile strain. Ic changes appreciably only in the first 5 percent tensile strain. For G. P. II zone containing single crystals, Iv in Fig. 4 shows little but scatter once the initial 5 percent strain is completed.

For crystals containing the transition precipitate θ' and the equilibrium precipitate θ, the Doppler behavior is dramatically different from that for G. P. zones as might be expected from the very different deformation mechanisms involved. For example, for θ' containing crystals, both Iv and Ic respond quite rapidly to tensile strain as shown in Fig. 5. Again, for crystals containing the equilibrium precipitate θ, Fig. 6 shows a lesser magnitude, but an equally rapid response than for θ'.

The main distinguishing feature we seem to be seeing is that the cutting of G. P. zones does not appreciably change the positron response, but the operation of Fisher-Hart-Pry[5] or Orowan[6] work hardening mechanisms definitely does cause a positron response. The reason suggested is that positrons trap at the dislocations which wrap around the θ' and θ particles, but do not respond very much to the cutting of G. P. zones by rigidly moving dislocations.

The second subject to be discussed is the hydrogen charging of metals[7]. Earlier work[8] in this laboratory showed a hydrogen-positron relationship in steel which was appropriate for the nondestructive detection of hydrogen embrittlement. In the subsequent work[8], nickel (after various amounts of cold work) was cathodically charged with hydrogen. The sharpness of the Doppler peak increased at first and to a greater extent the greater the amount of initial deformation. Following the initial sharpening, a broadening occurred. A mechanism which could explain this is one in which protons migrate to dislocations introduced by cold work and subsequently form gaseous hydrogen molecules which produce enough pressure to generate new dislocations at these locations. The broadening of the Doppler peak, following the initial narrowing, is attributed to protons reducing the attractive potential between positrons and dislocations. Figure 7 shows the undulating character of the positron-proton-dislocation relationship for two current densities for samples deformed 10.7 percent in tension.

A 70 percent cold rolled sample was cathodically charged for three hours and then measured as a function of time at 300°K. Figure 8 shows how P/W increased during this period. This is attributed in part to the diffusion of protons out of the sample. This would unscreen some dislocations and thus raise P/W. Another cause may be that protons detrapped from dislocations or delivered by dislocation short-cut diffusion to inclusions or grain boundary locations may combine to form H_2 and generate new dislocations by exerting pressure.

Figure 9 shows a schematic diagram of microhardness measurement directions on special samples. The central impression was made with a 1 kg load and the two orthogonal directions enabled 25 gram microhardness measurements to be made as a function of distance from the large impression with and without hydrogen charging. Figure 10 shows on the upper curve (H_1) how the microhardness varies with distance from a high dislocation density after charging and after a one hour anneal at 365°K (curve H_2); that is, with no charging.

Cathodic charging produced no change in the P/W shape factor of annealed Ni; yet, the microhardness of annealed Ni increased with charging as is seen by the right end of curve H_1 (higher than right end of curve H_2). This suggests that the P/W ratio was seeing an exact balancing between defect generation and defect screening by protons during charging. Yet, the existence of the defects could be seen via microhardness.

ACKNOWLEDGEMENTS

The authors wish to acknowledge the financial support of the Air Force Office of Scientific Research which made this work reported in this review possible.

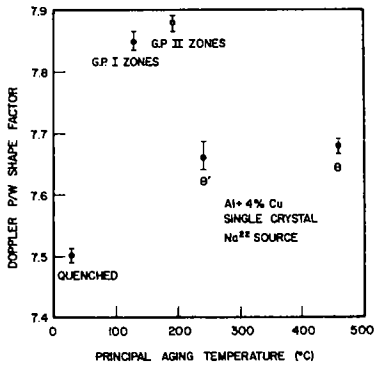

Fig. 1. Doppler P/W shape factors for an Al + 4 percent Cu single crystal in various aged states. Na^{22} positron source.

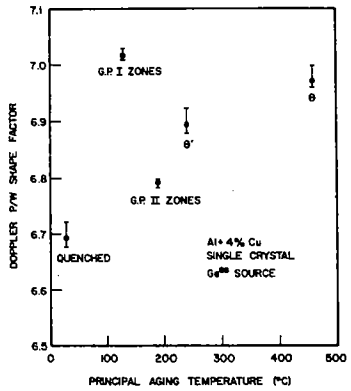

Fig. 2. Doppler P/W shape factors for an Al + 4 percent Cu single crystal in various aged states. Ge^{68} positron source.

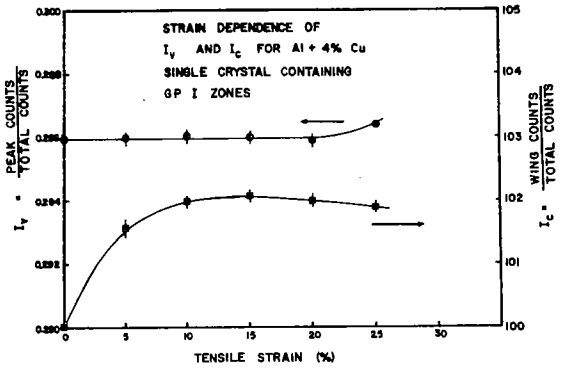

Fig. 3. Doppler peak to total (Iv) and wings to total (Ic) shape factors versus tensile strain for an Al + 4 percent Cu single crystal containing G. P. I zones.

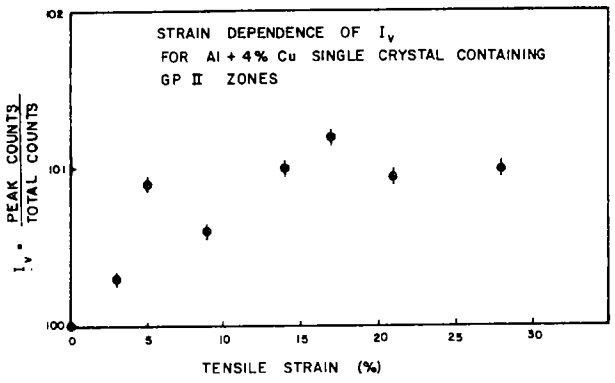

Fig. 4. Doppler peak to total (Iv) shape factor versus tensile strain for an Al + 4 percent Cu single crystal containing G. P. II zones.

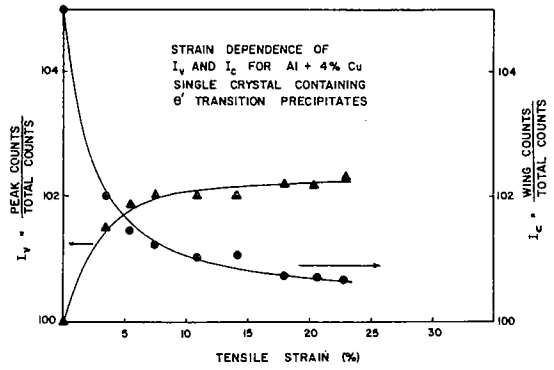

Fig. 5. Doppler peak to total (Iv) and wings to total (Ic) shape factors versus tensile strain for an Al + 4 percent Cu single crystal containing θ' transition precipitates.

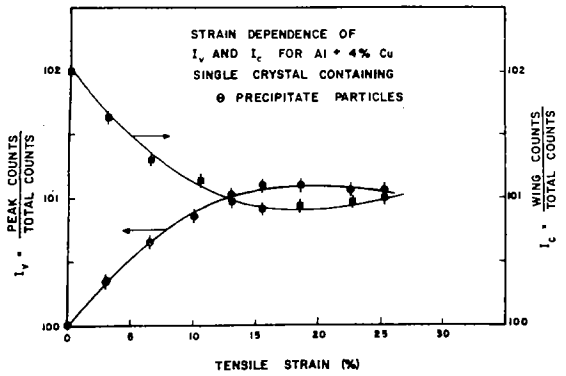

Fig. 6. Doppler peak to total (Iv) and wings to total (Ic) shape factors versus tensile strain for an Al + 4 percent Cu single crystal containing θ equilibrium precipitate particles.

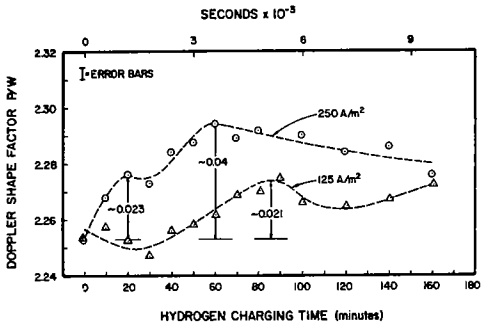

Fig. 7. Doppler peak to wings shape factor versus hydrogen charging time in polycrystalline nickel.

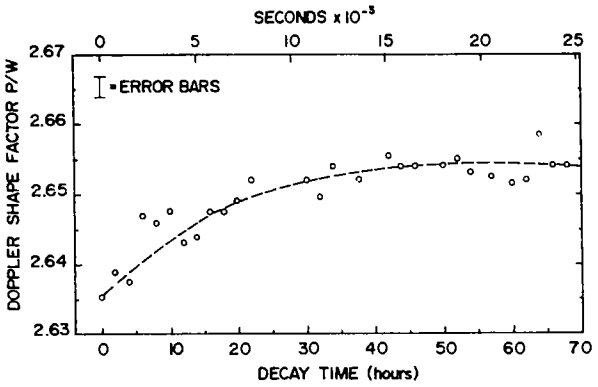

ig. 8. Doppler peak to wings (P/W) shape factor versus decay time at ambient following cathodic charging F hydrogen into nickel.

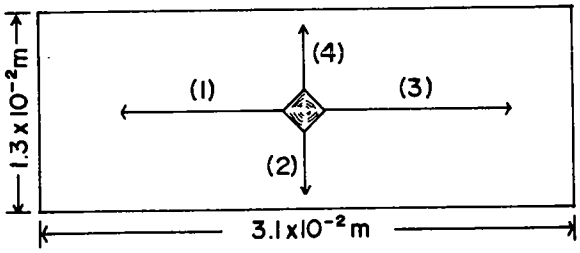

ig. 9. Microhardness measurement directions and sample size for results shown in Fig. 10. Paths 1 and 2 ›uld be used before and paths 3 and 4 after cathodic charging.

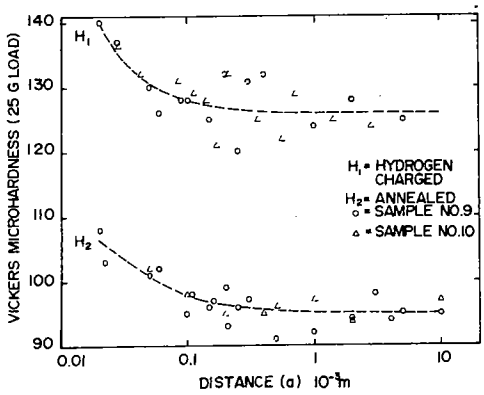

g. 10. Microhardness versus distance from a 1,000 gm impression before (curve H_2) and after (curve H_1) ıthodic charging of hydrogen into nickel.

References

1. M. L. Johnson, S. Panchanadeeswaran, S. Saterlie, and J. G. Byrne, Phys. Stat. Sol. (a) 42, 175 (1977).

2. S. Panchanadeeswaran, R. W. Ure, Jr., and J. G. Byrne, Phys. Stat. Sol. (a) 48, 83 (1978).

3. S. Panchanadeeswaran, unpublished results (1979).

4. J. G. Byrne, M. E. Fine, and A. Kelly, Phil. Mag. 6, 1119 (1961).

5. J. C. Fisher, E. W. Hart, and R. H. Pry, Acta. Met., 1, 336 (1953).

6. E. Orowan, A Symposium on Internal Stresses (London: Inst. of Metals), 451 (1948).

7. Po-We Kao, R. W. Ure, Jr., and J. G. Byrne, Phil. Mag. (a) 39, 517 (1979).

8. F. Alex, Ph.D. thesis, University of Utah (1976).